Sensors & Transducers, Vol. 27, Special Issue, May 2014, pp. 15-21

Sensors & Transducers

A Flexible Label-Free Biosensor Sensitive and Selective to TNF-α: Application for Chronic Heart Failure

[1] Abdoullatif BARAKET, [1] Michael LEE, [1] Nadia ZINE, [2] Nourdine YAAKOUBI, [3] Maria Giovanna TRIVELLA, [4] Abdelhamid ELAISSARI, [4] Monique SIGAUD, [1] Nicole JAFFREZIC-RENAULT, [1] Abdelhamid ERRACHID

[1] Institut des Sciences Analytiques (ISA), Université Lyon, Université de Claude Bernard Lyon 1, UMR 5280, 5 rue de la Doua, 69100 Villeurbanne, 6 France
[2] Université du Maine UMR CNRS 6613, rue Olivier Messiaen, 72085, LE MANS Cedex9, France
[3] CNR (Consiglio Nazionale Ricerche) Clinical Physiology Institute, Pisa, Italy
[4] Université de Lyon, Université Claude Bernard Lyon-1, CNRS, UMR 5007, LAGEP, F-69622 Villeurbanne, France
E-mail: a.baraket@gmail.com, abdelhamid.errachid@univ-lyon1.fr

Received: 31 December 2012 /Accepted: 22 November 2013 /Published: 26 May 2014

Abstract: Tumor necrosis factor-α (TNF-α) is a key pro-inflammatory cytokine that is characterized by elevated circulating levels for chronic heart failure (CHF) and left ventricular assisted device (LVAD) implantation patients, respectively. Therefore, a rapid and ease-of-use diagnostic tool is required to monitor LVAD patients at a high risk of mortality during early expression of an inflammatory storm. In this paper, we report on the quantitative electrochemical detection of human TNF-α with its corresponding antibody (Ab) immobilized onto the functionalized biosensor surface. The label-free biosensor was fabricated on a gold surface that was deposited on a flexible polyimide (PI) substrate. The interfacial properties of the functionalized flexible gold electrodes were evaluated by cyclic voltammetry (CV) in the presence of $Fe(CN)_6^{4-/3-}$ as the redox-active species. Afterwards, the electrochemical impedance spectroscopy (EIS) technique was used to determine the TNF-α concentrations. EIS results confirmed that the developed flexible biosensor can accurately detect TNF-α with a good sensitivity in the dynamic range of 0.1 pg/mL to 0.5 ng/mL. Overall, the developed flexible biosensor was easy to fabricate and the results demonstrate a good selectivity in the presence of other cytokines such as interleukin: (IL-10) and (IL-1). *Copyright © 2014 IFSA Publishing, S. L.*

Keywords: Tumor necrosis factor-α, Flexible gold electrodes, Electrochemical impedance spectroscopy.

1. Introduction

Cytokines are small protein molecules that are secreted in the course of immunologic and inflammatory responses. They function as intercellular signals and are produced by a variety of different cell types such as macrophages and T-(cells) to regulate both local and systemic inflammatory responses [1]. In the family of cytokines, dysregulation of tumor necrosis factor-α (TNF-α) secretions are implicated in a variety of diseases such as cancer [2].

The measurement of cytokine concentrations based on bio-recognition interactions, have been considered a major bio-analytical tool in the field of clinical diagnostics [3-5]. Various commonly available methods have been developed for the determination of cytokine concentrations, such as radioimmunoassay [6] and conventional enzyme-linked immunosorbent assay (ELISA) [7]. Unfortunately, these techniques require highly qualified personnel, complicated wash procedures, are expensive and time-consuming [8]. The limit of detection (LOD) of these standard immunoassays is typically in the range of 1-10 pg/mL for cytokines. For instance, H. Antonissen et al. [9] have reported a LOD = 9 pg/mL for TNF-α using multiplexed bead detection. In the same principle, Toedter et al [10] have also reported the lowest detectable level with LOD = 2.4 pg/mL for TNF-α using electrochemiluminescent technique.

In the last few years, TNF-α has been credited as a specific biomarker that is secreted as a response after left ventricular assist device (LVAD) transplantation for patients suffering from Heart Failure (HF) [11]. Consequently, measurements and analysis of cytokine TNF-α at small concentrations are very useful for clinicians and doctors. For this purpose, many assays which are more sensitive and specific for direct detection of TNF-α are clearly required. The label-free techniques are well suited for such application in which the expected variations of impedimetric properties occur when the target is perturbed at the sensing interface. As a sensitive and non-destructive technique, label-free electrochemical sensing methods based on electrochemical impedance spectroscopy (EIS) has recently received considerable attention for the characterization of the electrical properties in biological and chemical interfaces [12-19].

Silicon-based technologies are considered one of the most advanced fabrication processes to produce biosensors. However, flexible substrates based on polymers are a competitive alternative to inorganic materials such as silicon. In this study, flexible substrates were applied to, firstly, optimize all conditions for surface functionalization, antibody immobilization, and electrochemical characterization. Once optimized, the second stage of development will consist of a lab-on-a-chip for multiple cytokine detection to formulate a biomedical microelectromechanical systems (BioMEMS) device. Compared to a rigid substrate such as silicon, the flexible polymeric substrate has good optical properties, lower cost, and provides better flexibility regarding surface manipulation (chemically and mechanically). Recently, we and others have shown the development of rapid and inexpensive flexible biosensors using a polymer as a substrate material [20-23].

The aim of the present study is the examination of EIS properties of the TNF-α/anti-TNF-α interaction on gold deposited on polyimide (PI) flexible substrates. Cyclic voltammetry (CV) and EIS were used to fully characterize each step of the bio-surface constructs and the binding of TNF-α to its specific antibody (Ab) already immobilized onto functionalized gold electrodes. Based on an equivalent circuit representation of the developed biosensor, the relationship between charge transfer resistance (Rct) and the concentration of TNF-α is proposed. The fabrication and testing of the flexible biosensor are described next in a step by step process.

2. Experimental

2.1. Materials and Chemicals

Anti-human TNF-α /TNFSF1A monoclonal antibody (mAb), Recombinant Human TNF-α, Recombinant Human IL-10 and Recombinant Human IL-1α/IL-1F1 were all purchased from R&D Systems, France. Ethanol 96 %, N-hydroxysuccinimide (NHS), N-Ethyl-N′-(3-dimethylaminopropyl), carbodiimide (EDC), 16-mercaptohexadecanoic acid (MHDA), phosphate buffered saline (PBS), sodium ferrocyanide decahydrate ≥99 %, potassium ferricyanide (III), and ethanolamine (ETA) were purchased from Sigma-Aldrich, France. Polyimide Kapton (NH) 125 μm was purchased from Dupont, France.

2.2. Electrodes Fabrication

Gold was deposited onto PI substrates using physical vapor deposition (PVD). A titanium (Ti) layer was applied as an intermediate film to enhance the adhesion of gold onto the PI. Both metals were deposited within a clean room environment. First, the PI substrate was cleaned by rinsing with acetone, IPA, and deionized water successively, followed by drying with a stream of nitrogen (N_2). The PI substrate was then affixed within the introduction chamber of the PVD machine (Plassys MP 450) at 5.5×10^{-2} Torr. The PI sample was then moved in the deposition chamber and a vacuum of 16 mTorr was established. Argon plasma etching was processed with 0.15 W/cm² DC power for 2 min. This step for PI surface activation enhances metal PI adhesion. A thin Ti layer (20 ± 0.29 nm) was sputtered onto the PI substrate for 2 min (RF-Sputtering mode) at the same pressure. This was immediately followed by the gold layer deposition (200 ± 0.58 nm) using DC mode for 40 s. The thickness of gold (200 ± 0.58 nm) was measured using a mechanical profilometer (Veeco Dektak-8).

2.3. Immobilization of Antibodies

Electrodes were pre-cleaned with acetone, ethanol, and copious amounts of deionized water. Afterwards, the electrodes were incubated overnight

within a teflon cell in 800µL of pure ethanol containing 10 mM of MHDA at 4 °C. Consequently, self assembled monolayers (SAMs) of MHDA were formed onto the gold surface with carboxylic acid terminal groups projected away from the surface.

After SAMs formation, the electrode was rinsed with ethanol to remove any unbounded MHDA and dried under a N_2 flow.

The carboxylic acid groups of the SAMs were activated with a mixture of EDC (0.4 M) and NHS (0.1 M) in ethanol for 1hr at room temperature (24°C), as already described in [24, 25]. This activation enabled the bonding of the monoclonal antibody (mAb) through the acid-amine linkage. The functionalized electrodes were then rinsed with ethanol, dried with a stream of N_2, and immediately incubated in a solution of mAb-anti-TNF-α (10 mg/mL) in PBS buffer for 1hr at 4°C. Here, the mAb-TNF-α was immobilized onto the functionalized electrodes through the activated carboxylic acid and the amine groups provided from mAb's. Afterwards, residual activated carboxylic acid groups were blocked with 1 mM of ethanolamine diluted in PBS for 20 min at 24°C. This prevented non-specific binding. Finally, the biosensor was rinsed with PBS and used for EIS measurements. Fig. 1 depicts the bio-functionalization of the biosensor as detailed in the experimental.

2.4. Electrochemical Measurements

The electrochemical characteristics of the modified electrodes were measured using CV and faradaic impedance. Electrochemical measurements were performed in a conventional electrochemical cell containing a three electrode system using a VMP3 (Bio-logic-Science Instrumentation, France). The PI-based biosensor was diced into small pieces of 1.5 cm × 1 cm, sandwiched between the two parts of the Teflon cell, and tightened (Fig. 2). The chosen distance of 1.5 cm allows the connection of a gold electrode to the potentiostat (VMP3) from the outside part of the Teflon cell. Also, the distance of 1 cm was chosen to prevent leakage of the electrolyte solution between the gold and rubber ring. The biosensor surface that was exposed to the electrolyte was ~7 mm². A platinum (Pt) wire with a diameter of ~ 0.5 mm and a silver/silver chloride (Ag/AgCl) electrode were used as the counter and reference electrode, respectively. Both electrodes were purchased from Bio-Logic-Science Instrumentation, France.

CV measurements were performed in a mixture (1:1) of 5 mM $K_3[Fe(CN)_6]/K_4[Fe(CN)_6]$ as the redox probe in PBS (pH 7.4). The potential was swept between -0.4 V and 0.5 V (versus Ag/AgCl) at a rate of 100 mV/s.

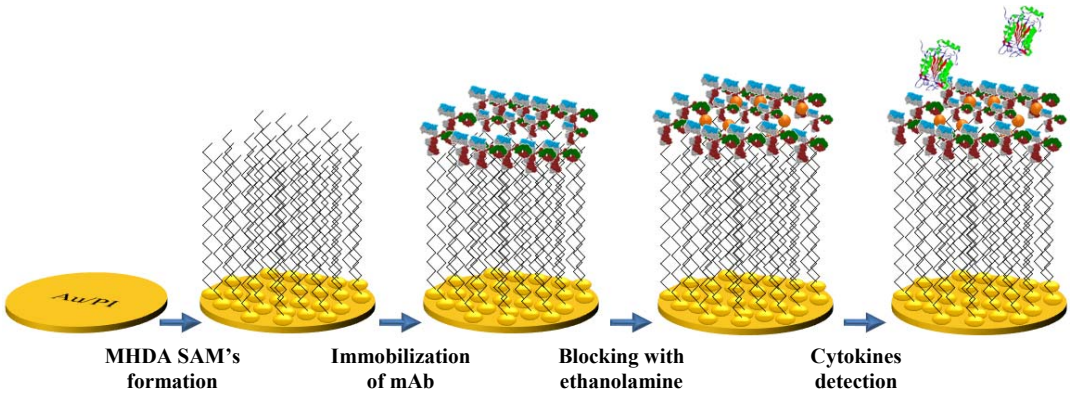

Fig. 1. Schematic representation of the mAb-TNF-α immobilization on a gold electrode modified with MHDA starting by: The formation of MHDA SAMs on a gold substrate; the activation of carboxylic acid functional groups with a solution of EDC/NHS; coupling the mAb-TNF-α to the activated SAMs through amino-acid bonding; blocking the residual activated groups with ethanolamine; and detection of the corresponding cytokine.

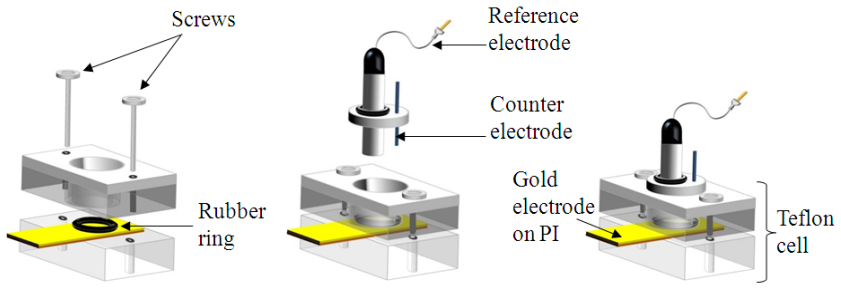

Fig. 2. Scheme (from left to right) showing all Teflon cell elements, which will be connected to the VMP3 for electrochemical measurement (CV and EIS).

2.5. Contact Angle Measurement (CAM)

CAM (Digidrop, GBX Scientific Instrument, France) was applied to characterize the gold substrates that were treated by MHDA and mAb-TNF-α. The measurements were analyzed with a droplet of 5µL of deionized water, for the untreated gold substrate and after each stage of the gold substrate treatment.

Impedance measurements were carried out in the same solution at ambient temperature in a frequency range from 100 mHz – 100 kHz, at a polarization potential of -0.1 V/ Ag/AgCl with a frequency modulation of 10 mV. The potential was fixed at -0.1 V. The modeling of the obtained EIS data were made by the EC-Lab software using the Randomize + Simplex method, with randomize stopped on 100,000 iterations and the fit stopped on 5,000 iterations. All electrochemical measurements were performed inside a Faraday cage.

3. Results and Discussions

3.1. Contact Angle Measurement

Water angle measurements were made to characterize the functionalized gold microelectrode on a PI substrate. The contact angle was 79.6 ± 1° for the bare gold microelectrode (Fig. 3a), which corresponds to literature angles of 80 ± 1° [26], whilst, the MHDA treated gold electrode was 35.9 ± 1° (Fig. 3b).

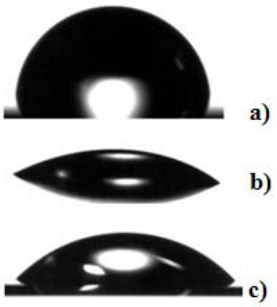

Fig. 3. Surface wettability for: a) bare gold, b) MHDA treated gold microelectrode, and c) immobilization of mAb-TNF-α onto the gold microelectrode.

3.2. Electrochemical Characterization of MHDA SAMs

CV is often used to study the compactness and the blocking effect of a SAMs modified electrode through a redox behavior of a reversible $Fe(CN)_6^{3-}$ /$Fe(CN)_6^{4-}$ pair [27,28]. Fig. 4a shows both oxidation and reduction peaks for the bare gold at ~ 0.263 V and 0.177 V, respectively. However, the redox peaks totally disappeared after the formation of SAMs onto the gold surface electrode (Fig. 4b and inset). This was attributed to the SAMs acting as an insulating layer that blocked the electron transfer at the electrode interface [29].

This alteration was due to the cathodic and anodic waves of the redox probe for the bare gold microelectrode when compared to the SAMs covered gold microelectrode curve, respectively.

This hydrophilic character proves the presence of carboxylic acid as the terminal group. This signifies that the MHDA was successfully chemisorbed on the gold microelectrode. After immobilization of the mAb-TNF-α on the SAMs of MHDA, the CAM measurement increased from 35.9 ± 1° to 47.6 ± 1° indicating that the mAb's were well bonded to the activated carboxylic acid due to its decreased hydrophilic nature (Fig. 3c).

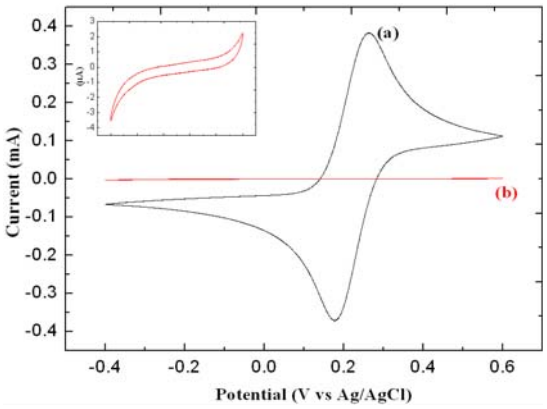

Fig. 4. CV for bare gold and mixed SAM electrodes in 5 mM K3[Fe(CN)6]/ K4[Fe(CN)6] in PBS (pH 7.4). Electrodes were scanned at a rate of 100 mV/s with (a) bare gold electrode and (b) mixed SAMs of MHDA covered electrode. This confirms the functionalization of the gold microelectrodes. (Inset shows the magnification of the curve (b)).

3.3. EIS Measurements

To evaluate the interaction of mAb-TNF-α/TNF-α based on the MHDA modified electrode, in terms of the sensitivity and selectivity, the biosensor was exposed to various human TNF-α antigen (Ag) concentrations. This was made in the presence of a reversible $[Fe(CN)_6]^{3-/4-}$ redox-active probe in PBS (pH 7.4). The interaction of the mAb-TNF-α/TNF-α or Ab-Ag was followed by EIS measurements for each TNF-α cytokine concentration. The output data were presented in the corresponding complex-plane impedance plots also known as a Nyquist plot (Fig. 5). For each concentration of TNF-α, the corresponding response in the Nyquist plot was presented as two semicircles (one at high frequency and other at low frequency). This indicates the existence of at most two relaxation processes in the studied system.

The equivalent electrical circuit, shown in Fig. 6 (inset), was used to adequately fit the data over the entire frequency range. Here, the circuit includes

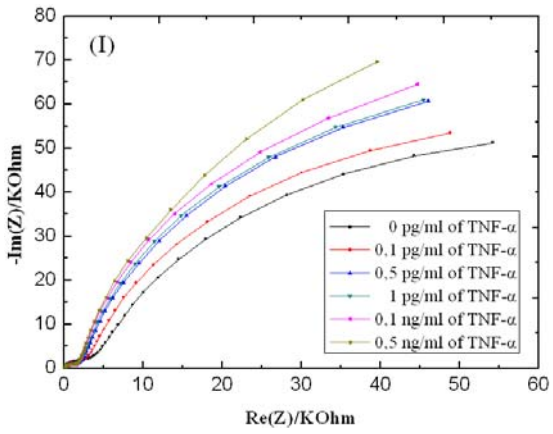

Fig. 5. Nyquist plot impedance (Zr vs. Zi: vs. SCE at 5 mM of $K_3[Fe(CN)_6]$/ $K_4[Fe(CN)_6]$ in PBS (pH 7.4) at various human TNF-α concentrations detected by the corresponding mAb: (▪) 0 pg/mL; (•) 0.1 pg/mL; (▲) 0.5 pg/mL; (▼) 1 pg/mL; (◄) 0.1 ng/mL; and (►) 0.5 ng/mL.

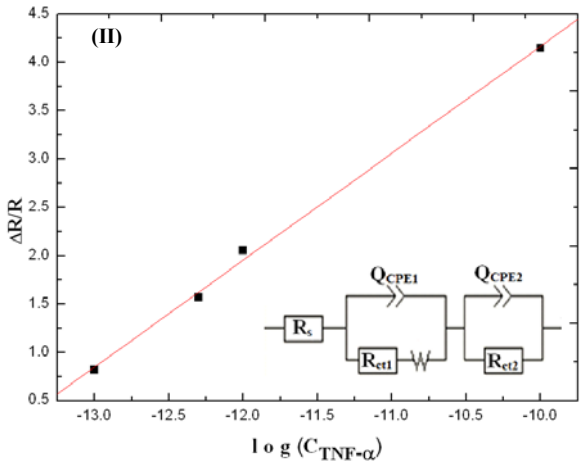

Fig. 6. The normalized transfer resistance of transfer charge vs. the log of human TNF-α concentrations. The parameter ΔR/R was given as (R_{ct2}-Ag - R_{ct2}-Ab)/R_{ct2}-Ab, where R_{ct2}-Ab represents the charge transfer resistance when Anti-TNF-α is immobilized on the SAM/Au electrode, and R_{ct2}-Ag corresponds to the charge transfer resistance at different TNF-α Ag concentrations.

six elements: the ohmic resistance of electrolyte solution, R_s; the constant phase element, Q_{CPE1}, reflecting the non-homogeneity of negative and positive charges at the gold electrode interface; the charge transfer resistance R_{ct1} which reflects the direct charge transfer to and from the gold surface (this corresponds to the first small semicircle of the Nyquist plot), the second R_{ct2} describes the electron transfer through the immobilized substances, including SAMs, mAb's, and Ag's (this correspond to the second semicircle of the Nyquist plot) and, finally, the second Q_{CPE2} which reflects the non-homogeniety of the charges at the biolayer interface in the presence of the large protein molecules.

In Fig. 5, the EIS results show increasingly large R_{ct2} as the Ag concentration was increased. Therefore, the biolayer based of anti-TNF-α was nonconductive, the immobilization of anti-TNF-α formed a steric hindrance which blocked the electron transfer of $[Fe(CN)_6]^{3-/4-}$. As the TNF-α protein interacted with anti-TNF-α, a further increase in R_{ct2} was observed (increase in shift between the semicircles of the Nyquist plot).

Table 1 shows the simulated parameters from the impedance data obtained for each TNF-α concentration. The R_{ct2} was found to be the most sensitive to the changes in concentration and it was, thus, selected as the relevant parameter to monitor the sensitivity and selectivity of the developed biosensor. Fig. 6 shows a good linear relationship between ΔR/R and the TNF-α protein concentrations ((R_{ct2}-Ag - R_{ct2}-Ab)/R_{ct2}-Ab) = 15.237+1.107 log CTNF-α) which was found to be in the dynamic range of 0.1 pg/mL to 0.5 ng/mL. In this study, the LOD was determined at 0.1 pg/mL.

This shows the high sensitivity of the developed biosensor when compared to other sensors using conventional techniques such as ELISA [30-31].

The sensitivity and specificity of the developed biosensor was also studied in the presence of other biomarkers (interleukin-1 (IL-1) and interleukin-10 (IL-10)). Here, the same experimental process of anti-TNF-α immobilization was applied and followed by EIS measurements in the presence of IL-1 and IL-10 successively. Fig. 6 illustrates the high selectivity and sensitivity of the biosensor toward TNF-α. The response of the biosensor was ~ 9 times higher in the presence of only 0.1 pg/mL of TNF-α when compared to 1 ng/mL of IL-1 or IL-10. By increasing the concentration of the human TNF- α, the biosensor always showed a good selectivity and sensitivity of the Ag when compared to the other inactive cytokines. The weak signal detected for IL-1 or IL-10 for each concentration was due to the non-specific binding of these biomarkers and, therefore, the level of interference of these inactive Ag's was minimal and non-attributable to the detection of human TNF-α.

Table 1. All resistance values after fitting of each Nyquist plot semicircle. Errors were given by the same EC-Lab software.

$[C_{TNF-α}]$ pg/mL	Rs (Ohm)	R_{ct1} (Ohm)	R_{ct2} (Ohm)
0	53.2 ± 0.3	2,863 ± 5	81,774 ± 47
0.1	54.8 ± 0.3	2,029 ± 4	97,355 ± 806
0.5	58.7 ± 0.3	1,656 ± 3	129,471 ± 106
1	65.2 ± 0.3	1,570 ± 3	134,277 ± 107
100	54.8 ±0.3	1,465 ± 2	149,230 ± 112
500	58.9 ± 0.3	1,476 ± 2	190,357 ± 126

Finally, the application of this current work has demonstrated the potential for applying this biosensor in a clinical environment. The dynamic range between 0.1 pg/mL to 0.5 ng/mL is sensitive to minute concentrations of TNF-α, while also large enough to accommodate a cytokine storm. For instance, in a study by Caruso et al [11], after LVAD implantation the TNF-α plasma levels increased for survivors and non-survivors between a range of ~ 1.5 – 150 pg/mL during one month of analysis, where patients are at the most critical condition for multiple organ failure syndrome (MOFS). These results were analyzed by the gold standard of ELISA. Here, by a label free method, the possibility of real-time results will undoubtedly improve the therapeutic intervention the patient can acquire before the off-set of MOFS.

4. Conclusions

A label-free, highly sensitive, low cost and fast EIS flexible biosensor for detection of TNF-α was developed. The mAb-TNF-α was immobilized onto a functionalized gold layer that was deposited onto a flexible PI substrate. The developed biosensor can detect human TNF-α with a good sensitivity in the range of 0.1 pg/mL to 0.5 ng/mL. The level of interference attributable to non-specific binding was minimal as a good selectivity was observed in the presence of other inactive cytokines (IL-10 and IL-1). This flexible biosensor is a promising bio-analytical tool for accurate quantification of TNF-α when applied here with commercial cytokines. Future work will concentrate on the analysis of plasma samples for cytokine detection that will eventually be applied to measure plasma samples of patients after cardiac surgery with LVAD implantation.

Acknowledgements

This work was funded by the European Communities Seventh Framework Programme (FP7/2007-2013) under the grant agreement No. 248763 (SensorART) and FP7-PEOPLE-2012-IRSES under the grant agreement No. 318053 (SMARTCANCERSENS) and SPS (NUKP.SFPP984173) NATO project.

References

[1]. B. K. Pedersen, T. C. A. Akerstrom, A. R. Nielsen, P. C. Fischer, Role of myokines in exercise and metabolism, *Journal of Applied Physiology*, Vol. 103, 2007, pp. 1093-1098.

[2]. J. Lin, D. Ziring, S. Kim, M. Wong, Y. Korin, E. Reed, D. Gjertson, R. R. Singh, TNFα blockade in human diseases: An overview of efficacy and safety, *Clinical Immunology,* Vol. 126, 2008, pp. 13-30.

[3]. M. Y. Liu, A. M. Xydakis, R. C. Hoogeveen, P. H. Jones, E. O. Smith, K. W. Nelson, C. M., Multiplexed analysis of biomarkers related to obesity and the metabolic syndrome in human plasma, using the Luminex-100 system, Ballantyne, *Clinical Chemistry*, Vol. 51, 2005, pp. 1102-9.

[4]. Q. Fu, J. Zhu, J. E. Van Eyk, Comparison of multiplex immunoassay platforms, Clinical Chemistry., Vol. 56, 2010, pp. 314-318.

[5]. L. Song, D. W. Hanlon, L. Chang, G. K. Provuncher, C. W. Kan, T. G. Campbell, D. R. Fournier, E. P. Ferrell, A. J. Rivnak, B. A. Pink, K. A. Minnehan, P. P. Patel, D. H. Wilson, M. A. Till, W. A. Faubion, D. C. Duffy, Single molecule measurements of tumor necrosis factor α and interleukin-6 in the plasma of patients with Crohn's disease, *Journal of Immunological Methods,* Vol. 372, 2011, pp. 177-186.

[6]. O. Stannus, G. Jones, F. Cicuttini, V. Parameswaran, S. Quinn, J. Burgess, C. Ding. Circulating levels of IL-6 and TNF-α are associated with knee radiographic osteoarthritis and knee cartilage loss in older adults*, Osteoarthritis and Cartilage*, Vol. 18, 2010, pp. 1441-1447.

[7]. C. Ruffolo, M. Scarpa, D. Faggian, A. Pozza, F. Navaglia, R. D'Incà, P. Hoxha, G. Romanato, L. Polese, G. C. Sturniolo, M. Plebani, D. F. D'Amico, I. Angriman, Cytokine network in rectal mucosa in perianal Crohn's disease: Relations with inflammatory parameters and need for surgery, *Inflammatory Bowel Diseases,* Vol. 14, 2008, pp. 1406-1412.

[8]. X. Ao, R. F. Retundo, D. J. Loegering, J. A. Stenken, In vivo microdialysis sampling of cytokines produced in mice given bacterial lipopolysaccharide, *Journal of Microbiological Methods,* Vol. 62, 2005, pp. 327-336.

[9]. C. Heijmans-Antonissen, F. Wesseldijk, R. J. Munnikes, F. J. Huygen, P. van der Meijden, W. C. Hop, H. Hooijkaas, F. J. Zijlstra, Multiplex Bead Array Assay for Detection of 25 Soluble Cytokines in Blister Fluid of Patients with Complex Regional Pain Syndrome Type 1, *Mediators of Inflammation*, Vol. 1, 2006, pp. 1-8.

[10]. G. Toedter, K. Hayden, C. Wagner, C. Brodmerkel, Simultaneous Detection of Eight Analytes in Human Serum by Two Commercially Available Platforms for Multiplex Cytokine Analysis, *Clinical and Vaccine Immunology*, Vol. 15, Issue 1, 2008, pp. 42-48.

[11]. R. Caruso, S. Trunfio, F. Milazzo, J. Campolo, De R. Maria, T. Colombo, M. Parolini, A. Cannata, C. Russo, R. Paino, M. Frigerio, L. Martinelli, O. Parodi, Early expression of pro- and anti-inflammatory cytokines in left ventricular assist device recipients with multiple organ failure syndrome, *American Society for Artificial Internal Organs,* Vol. 56, 2010, pp. 313-318.

[12]. E. Prats-Alfonso, X. Sisquella, N. Zine, G. Gabriel, A. Guimera, F. J. del Campo, F. J. R. Villa, A. H. Eisenberg, M. Mrksich, A. Errachid, J. Aguilo, Cancer Prognostics by Direct Detection of p53-Antibodies on Gold Surfaces by Impedance Measurements, Albericio F, *Small*, Vol. 8, Issue 13, 2012, pp. 2106-2115.

[13]. M. Lee, Z. Zine, A. Baraket, M. Zabala, F. Campabadal, R. Caruso, M. G. Trivella, N. Jaffrezic-Renault, A. Errachid, A novel biosensor based on hafnium oxide: Application for early stage

detection of human interleukin-10, *Sensors and Actuators B,* Vol. 175, 2012, pp. 201-207.
[14]. D. Caballero, E. Martinez, J. Bausells, A. Errachid, J. Samitier. Impedimetric immunosensor for human serum albumin detection on a direct aldehyde-functionalized silicon nitride surface, *Analytica Chimica Acta,* Vol. 720, 2012, pp. 43-48.
[15]. M. Hnaien, F. Lagarde, J. Bausells, A. Errachid, N. Jaffrezic-Renault, A new bacterial biosensor for trichloroethylene detection based on a three-dimensional carbon nanotubes bioarchitecture, *Analytical and Bioanalytical Chemistry,* Vol. 400, 2011, pp. 1083-1092.
[16]. Z. M. Baccar, D. Caballero, R. Eritja, A. Errachid, evelopment of an impedimetric DNA-biosensor based on layered double hydroxide for the detection of long ssDNA sequences, *Electrochimica Acta*, Vol. 74, 2012, pp. 123-129.
[17]. M. Hnaien, S. Bourigua, F. Bessueille, J. Bausells, A. Errachid, F. Lagarde, N. Jaffrezic-Renault, Impedimetric microbial biosensor based on single wall carbon nanotube modified microelectrodes for trichloroethylene detection, *Electrochimica Acta*, Vol. 56, 2011, pp. 10353-10358.
[18]. S. Bourigua, M. Hnaien, F. Bessueille, F. Lagarde, S. Dzyadevych, A. Maaref, J. Bausells, A. Errachid, N. Jaffrezic-Renault, Impedimetric immunosensor based on SWCNT-COOH modified gold microelectrodes for label-free detection of deep venous thrombosis biomarker, *Biosensors & Bioelectronics,* Vol. 26, 2010, pp. 1278-1282.
[19]. I. A. M. de Oliveira, F. Vocanson, J. P. Uttaro, Z. Asfari, C. A. Mills, J. Samitier, A. Errachid. Characterization of a Self-Assembled Monolayer Based on a Calix[4]Crown-5 Derivate: Fabrication of a Chemical Sensor Sensitive to Calcium, *Journal of Nanoscience and Nanotechnology,* Vol. 10, 2010, pp. 413-420.
[20]. A. Baraket, M. Lee, N. Zine, M. Sigaud, N. Yaakoubi, M. G. Trivella, M. Zabala, J. Bausells, N. Jaffrezic-Renault, A. Errachid, Diazonium modified gold microelectrodes onto polyimide substrates for impedimetric cytokine detection with an integrated Ag/AgCl reference electrode, *Sensors and Actuators B,* Vol. 189, 2013, pp. 165-172.
[21]. M. Kuphal, C. A. Mills, H. Korri-Youssoufi, Polymer-based technology platform for robust electrochemical sensing using gold microelectrodes, J. Samitier, *Sensors and Actuators B*, Vol. 161, 2012, pp. 279-284.
[22]. A. Baraket, M. Lee, N. Zine, N. Yaakoubi, M. G. Trivella, M. Zabala, J. Bausells, N. Jaffrezic-Renault., A. Errachid, Cytokine Detection using Diazonium Modified Gold Microelectrodes Onto Polyimide Substrates with Integrated Ag/AgCl Reference Electrode, *Procedia Engineering*, Vol. 47, 2012, pp. 1181-1184.
[23]. A. Baraket, M. Lee, N. Zine, F. Besseuille, N. Yaakoubi, M. G. Trivella, J. Bausells, M. Zabala, N. Jaffrezic-Renault, A. Errachid, A highly sensitive biosensor for detecting TNF-alpha cytokine to predict the biocompatibility of transplanted organs, *International Journal of Artificial Organs*, Vol. 34, 2011, pp. 661-662.
[24]. M. Hnaien, F. Lagarde, J. Bausells, A. Errachid, N. Jaffrezic-Renault, A new bacterial biosensor for trichloroethylene detection based on a three-dimensional carbon nanotubes bioarchitecture, *Analytical and Bioanalytical Chemistry*., Vol. 400, 2011, pp. 1083-1092.
[25]. D. Caballero, M. Pla-Roca, F. Bessueille, C. A. Mills, J. Samitier, A. Errachid, Atomic Force Microscopy Characterization of a Microcontact Printed, Self Assembled Thiol Monolayer for Use in Biosensors, *Analytical Letters,* Vol. 39, 2006, pp. 1721-1734.
[26]. F. Bessueille, M. Pla-Roca, C. A. Mills, E. Martinez, Samitier J, A. Errachid, Submerged Microcontact Printing (SμCP): An Unconventional Printing Technique of Thiols Using High Aspect Ratio, Elastomeric Stamps, *Langmuir*, Vol. 21, 2005, pp. 12060-12063.
[27]. C. S. Chen, K. N. Chang, Y. H. Chen, C. K. Lee, B. Y-J. Lee, A. S-Y Lee, Development of a label-free impedance biosensor for detection of antibody–antigen interactions based on a novel conductive linker, *Biosensors & Bioelectronics,* Vol. 26, 2011, pp. 3072-3076.
[28]. A. E. Radi, X. Munoz-Berbel, V. Lates, and J. L. Marty, Label-free impedimetric immunosensor for sensitive detection of ochratoxin A, *Biosensors & Bioelectronics*, Vol. 24, 2009, pp. 1888-1892.
[29]. Y. Liu, M. Yang, Z. Zheng, and B. Zhang, Tailoring the electrochemical property of self-assembled monolayer of 16-mercaptohexadecanoic acid on gold (1 1 1) electrode with covalently coupling ethylene diamine, *Electrochemistry communication*, Vol. 7, 2005, pp. 344-348.
[30]. A. Qureshi, Y. Gurbuz, and J. H. Niazi, Biosensors for cardiac biomarkers detection: A review, *Sensors and Actuators B,* Vol. 171, 2012, pp. 62-76.
[31]. T. S. Pui, P. Kongsuphol, S. K. Arya, and T. Bansal, Detection of tumor necrosis factor (TNF-α) in cell culture medium with label free electrochemical impedance spectroscopy, *Sensors and Actuators B*, Vol. 181, 2013, pp. 494-500.
